Numerical Analysis of Fire Resistance Tests of Press-formed Steel Columns (BCP325)

by

Takeshi Okabe[1] and Mamoru Kohno[2]

ABSTRACT

A numerical simulation of the fire resistance test of large steel columns is presented. The experimental investigation into the fire resistance properties of axially loaded large steel box columns was described in References [1, 2] by the authors. In this paper, a procedure for a one-dimensional finite element of nonlinear numerical analysis was applied to simulate thermal deformation, described as an elastic-plastic-creep, of steel columns as they are subjected to high temperatures. The results of the calculations clearly show that numerical analysis can be used to provide accurate predictions of the deformation characteristics of columns at high temperatures when an appropriate mechanical model and creep strain data of steel materials at high temperatures are used.

KEYWORDS: Steel column, Press formed, Creep deformation, Fire resistance test, Tall building

1. INTRODUCTION

Few full-scale fire resistance tests applying actual axial forces have been conducted on steel columns used for tall buildings, and the fire safety of such columns is not thoroughly understood. One of the authors conducted loaded fire resistance tests of full-scale square steel tubes which were welded, assembled, and press formed. The results showed that the steel columns retained high heat resistance when their fire protection was sound but that compromised fire protection caused sharp drops in fire ratings [1, 2].

The authors also simulated the loaded fire resistance tests of weld-assembled square steel tube columns (Series A of Reference [1]) by a numerical analysis in which the behaviors of steel at high temperatures were considered. The results verified the analytical and physical experimental methods [3]. The numerical analysis, in which the behaviors of steel at high temperatures were considered, was shown to be effective in predicting the behaviors of the columns during loaded fire resistance tests, but creep data of steel at high temperatures need to be corrected for accurate behavior prediction.

This paper, a supplement to Reference [3], describes a simulation analysis of thermal elastic-plastic-creep deformation using the one-dimensional finite element method, which was conducted to reproduce the high axial-force loaded fire resistance tests (Series B) of cold press-formed square steel tube columns described in Reference [2] and to compare the experimental and analytical results.

This study is valuable since few tests have been conducted by applying loads and heat to full-size press-formed square steel tube columns until they collapse. In addition, as indicated in Reference [3], creep properties of steel at high temperatures are crucial for simulating the deformation behaviors of steel columns in detail. In this study, a numerical analysis was conducted using experimental creep data of steel to examine the validity of the method used for a simulation of the experimental behavior of steel columns at high temperatures.

This study aims to provide basic data and information about loaded fire resistance tests

1 Assoc. Prof., Graduate School of Science and Technology, Kumamoto University, Kumamoto-shi, Kumamoto-ken 860-8555, Japan

2 Research Coordinator for Quality Control of Building, Building Department, National Institute for Land and Infrastructure Management, Tsukuba-shi, Ibaraki-ken 305-0802, Japan

and numerical analyses to enhance fire safety in the design of buildings.

2. LOADED FIRE RESISTANCE TEST OF PRESS-FORMED SQUARE STEEL TUBE COLUMNS

An overview of the loaded fire resistance tests (Series B) conducted in Reference [2] is shown in Fig. 1 and Table 2, and the specifications of the specimens are shown in Table 1. The mechanical properties of the steel in the mill-sheet are shown in Table 3.

A high-performance column furnace at the Building Research Institute of Japan was used for the experiments. Press-formed square steel columns, BCP325, were used for test specimens. Two of the four columns were fabricated by using JIS G 3136 SN490B grade steel (conventional steel), and the remaining two columns were made of JIS G 3136 SN490B FR (fire-resistant) grade steel. The specified design strength is 325 MPa for both grades. The four columns had identical geometrical dimensions: the length was 4.3 m, the cross-section was 600 mm^2, and the plate thickness was 28 mm.

The columns were coated with a fire protection made of a ceramic fiber blanket which is a 1-hour rated protection material. According to the estimation in Reference [2], the columns corresponded to those used for the lowest stories of high-rise buildings of about 40 stories.

In the experiment, thermocouples were installed at the levels and positions shown in the middle figure of Fig. 1, and central compressive load was applied with the two spheres. As shown in Table 2, axial forces equal to 0.6 times and 1.0 times the long-term allowable axial force of the column were applied. Heat was applied along the standard fire temperature curve (ISO-834) and the temperature curve of hydrocarbon combustion. By the end of the experiment, all specimens showed buckling collapse.

3. METHODS OF NUMERICAL ANALYSIS

As in Reference [3], a method of thermal elastic-plastic creep deformation analysis by the one-dimensional finite element method was used. The analysis was based on a finite displacement formulation of the one-dimensional finite element procedure proposed by Fujimoto et al. [4] and was modified for thermal elastic-plastic creep deformation analysis [5, 6] by incorporating a mechanical model of steel at high temperatures [7].

The analytical method assumed that planes were retained and did not consider local buckling and lateral buckling. The members were divided into beam elements along the member axis. The cross-section of the column was divided along the center line of plate elements into small segments, and the areas of small elements were concentrated in the center of the segments. In the segments, both stress and strain were assumed to be uniform.

The analytical method used is a combined non-linear analysis method that simultaneously considers geometrical and material non-linearity. The method has been shown to be valid in past studies [11-14].

3.1 Analytical Model

The analytical model of the steel columns in the test apparatus is shown in the right figure in Fig. 1. In the column furnace, a column is a pin supported by two spheres at the top and bottom ends of a loading system. The buckling length of column specimens was 4.6 m. In the analytical model shown in Fig. 1, the columns were assumed to have the initial crookedness of a sinusoidal wave with a central value of $L/1000$, where L is the length of the columns. The model was divided along the length of the column into 44 beam elements, and the cross-section was divided into 22 elements as shown in Fig. 2.

In analyzing the columns, the axial loads were maintained at a constant level, and the heating time was increased by increments. The analysis continued until an equilibrium solution could no longer be found, signifying that the columns had failed. As the creep effect is a transient phenomenon, a transient analysis was carried out for a more realistic modeling of steel columns.

3.2 Temperature Distribution Model

In the experiment described in Reference [2], the temperature of column specimens was measured at nine sections (Levels A to I) using thermocouples (Fig. 1). Of the sections, the temperature was measured on both the surface and the back of the sections on Levels C, E, and G and was measured only at the surface on the other levels.

In this analysis, the surface temperature measured during the experiment was assumed to be the temperature in the middle of the plate thickness of the steel tube since the surface temperature was measured throughout the specimen and differed little from the temperature at the back, except at the corners, where it differed by 20 to 30 °C. Temperatures between the measured values were linearly interpolated along the sectional direction by assuming that the temperature distribution along the plate thickness direction was uniform and that temperature changed linearly along the length of the column.

3.3 Model of Steel Behaviors at High Temperatures

In order to model the behaviors of steel at high temperatures, the relationship between the stress and strain of steel at a certain temperature, a creep equation at high temperatures, and an equation of thermal expansion should be known [7].

3.3.1 Relationship between Stress and Strain of Steel at a Certain Temperature

In References [1] and [2], static tensile tests were conducted, and the stress-strain curves at ambient temperature, 400 °C, 500 °C, 600 °C, and 700 °C were obtained. In order to represent these stress-strain curves mathematically, Eqs. (1) and (2) were adopted (Fig. 3). The yield plateau in the stress-strain relationship of conventional steel SN490B is expressed by Eq. (1) in Fig. 3, and the other curve sections are expressed by Eq. (2).

The coefficients in Eqs. (1) and (2) were obtained directly by applying the least squares method to the digitalized stress-strain data. Since fire-resistant steel SN490B-FR showed no clear yield plateau even at ambient temperature, the relationship at all temperatures was expressed by Eq. (2). Thus, SN490B needed six coefficients, and SN490-FR needed four coefficients.

3.3.2 Effects of Cold Press Forming

Cold press forming is likely to cause changes in the stress-strain relationships of steels and increase their strength. However, no experimental studies have been conducted on the effects of cold press forming at high temperatures. In this study, the effects of cold press forming on the stress-strain relationships determined in Section 3.3.1 were handled in the following manner.

To show a trend of plastic processing erasing the yield plateau, the data for ordinary steel at 200 °C, shown in Table 4, were obtained from the data of SN490B at 300 °C, given in Reference [14], since the studies described in References [1, 2] did not obtain the stress-strain relationship of SN490B at temperatures below 400 °C.

The stress-strain curves drawn using the data from Table 4 are shown in Fig. 4. In general, for steel plates not subjected to plastic processing, the yield stage disappears at temperatures above 200 °C. On the other hand, the yield plateau in Fig. 4 disappeared at 100 °C. Since tensile tests of the fire-resistant steel resulted in a curved relationship between stress and strain, the disappearance of yield stage by plastic processing was not considered.

To consider the increases in strength by cold press forming, values 1.1 times larger than the yield strength values obtained by tensile tests were used for the structural calculations.

Cold press forming causes changes in the quality of materials at corners and has been reported to increase the yield point up to 1.4 to 1.6 from that of flat plate sections [9] although the value should differ by the degree of processing. Since corners account for less than 30% of the entire sectional area of a square steel tube, the mean yield strength of the entire section should be less than 1.15 times larger than that of the original flat steel plate.

In the calculations, the authors decided to use values 1.1 times larger than the yield strength of the original steel plates. Figs. 4 and 5 show the stress-strain relationships calculated using values 1.1 times larger than the yield strength of the original steel plates and the data given in Tables 4 and 5.

3.3.3 Creep-strain Equation at High Temperatures

The creep-strain equation at high temperatures should, in principle, be determined by conducting creep tests of steel column specimens at high temperatures and processing the data as for a stress-strain relationship. However, because creep tests at high temperatures require time, labor, and advanced skills, they are difficult to conduct. In this study, data of past studies were used [8, 10].

In References [8] and [10], the results of creep tests at high temperatures of SM50A and NSFR490A, respectively, were approximated using the least squares method to determine the coefficients of Eq. (3):

$$\varepsilon_c = 10^{a/T+b}(\sigma/9.81)^{c/T+d}\,t^{eT+f} \qquad (3),$$

where ε_c is creep strain (%), t is time (minutes), σ is stress (N/mm2), and T is absolute temperature (K). The material constants of SM50 were as follows: $a = -8.48 \times 10^3$, $b = 4.50$, $c = 3.06 \times 10^3$, $d = 2.28 \times 10^{-1}$, $e = 2.00 \times 10^{-3}$, $f = -1.10$.

The material constants of NSFR490A were $a = -4.205 \times 10^4$, $b = 37.615$, $c = 1.407 \times 10^4$, $d = -9.264$, $e = -1.584 \times 10^{-4}$, $f = 0.851$.

Since no experimental studies have been conducted on the creep strain of SN490B at high temperatures, the creep-strain equation of SM50A, which should have similar creep properties, was used.

To examine the accuracy of the creep-strain equation (Eq. (3)), the time history of the term of time t^{eT+f} in Eq. (3) is shown in Fig. 6, and the creep-strain curves of SM50 and NSFR490A, given by References [8] and [10], are shown in Fig. 7. In Fig. 7, the dashed lines show the experimental values of the creep tests at high temperatures, and the solid lines show the values calculated using Eq. (3). The stress levels in Fig. 7 were converted into SI units. Fig. 6 shows the basic form of the term of time t^{eT+f} in the creep-strain equation (3) at certain high temperatures (400 to 700 °C), and Fig. 7 shows the quantitative correlation between the experimental and calculated results.

As shown in Fig. 6, the primary creep decreased and the secondary creep increased in SM50 steel as the temperature rose from 400 to 600 °C. On the other hand, NSFR4909A showed large secondary creep regardless of temperature.

As shown in the upper figure of Fig. 7, the calculated values of SM50 were slightly larger than the experimental values at 450 °C but reproduced well the increases in the primary creep. At 500 °C, the experimental results showed large secondary creep, although the calculated results still showed the primary creep to be larger than the secondary creep. The relationship as a whole showed experimental values taking over the calculated values in the middle of the course. At 550 °C and with large stresses, the calculated strain values were smaller than the experimental values.

On the other hand, NSFR490A in the bottom figure of Fig. 7 showed smaller calculated values at 550 °C since the experimental values, which resulted in large primary creep, were approximated using a function that resulted in large secondary creep. At 600 °C and 650 °C, the relationship between the experimental and calculated values was complicated. Even at the same temperature, the relationship was reversed by stress level, and the experimental values showed tertiary creep.

Since the correlation between the experimental and calculated creep values of the steels at high temperatures was complicated, their qualitative and quantitative correlations need to be thoroughly understood in order to use the values for calculations.

3.3.4 Equation of Thermal Expansion

$$\varepsilon_T = 5.04\times10^{-9}\theta^2 + 1.13\times10^{-5}\theta \qquad (4),$$

where θ is temperature (°C).

4. RESULTS AND DISCUSSION

4.1 Tests of Conventional Steel Columns B-CS06 (Fig. 8) and B-CS10 (Fig. 9)

The conventional steel column B-CS06 (Fig. 8) was heated by the ISO 834 standard fire temperature curve, and B-CS10 (Fig. 9) was heated by the hydrocarbon fire curve. The existing load ratios to sustained allowable load were 0.6 for B-CS06 and 1.0 for B-CS10. The mean axial stress values, which were calculated by simply dividing the axial load by sectional area, were 143.3 N/mm^2 and 236.5 N/mm^2, respectively.

The upper figures in Figs. 8 and 9 show the steel temperatures measured at points on Level E (experimental values), the middle figures show column elongations (experimental and calculated values), and the bottom figures show the deflection W at the middle of the columns (calculated values). To examine the effects of the accuracy of the creep-strain equation at high temperatures, three cases were calculated using values 40% larger and smaller than the value determined by Eq. (3). In the middle figures, open circles denote the experimental values, solid lines denote values calculated by considering creep at high temperatures, and dashed lines denote calculations made by disregarding the creep strain.

As shown in the upper figures, the temperature distribution was almost uniform throughout the cross-section when the columns were heated. The steel temperatures of B-CS06 and B-CS10 rose almost linearly by 150 °C to 200 °C per hour.

The calculated values for B-CS06 with consideration of creep strain at high temperatures (solid line) reproduced the experimental values very accurately. The 40% fluctuation of the creep strain at high temperatures corresponded to a collapse time of about 10 minutes. The values calculated by disregarding creep strain at high temperatures (dashed lines) continued rising until immediately before the collapse and differed from the actual contraction observed in the experiment.

The results show that, at high temperatures, creep strain needs to be considered to correctly reproduce the actual behaviors during collapse (contraction of displacement U) and that disregarding creep strain results in predicting collapse time on the dangerous side.

The calculated values for B-CS10 (Fig. 9) with consideration of creep strain at high temperatures (solid line) reproduced the experimental results except that the calculated contraction behavior occurred slightly earlier than the actual contraction (open circles). Since the 40% reduction in creep strain at high temperatures matched the experimental values, Eq. (3) for calculating creep strain at high temperatures may tend to overestimate the creep strain of SN steel under large stresses.

The values calculated by disregarding creep strain at high temperatures (dashed lines) continued rising until immediately before the collapse and differed from the actual contraction observed in the experiment, suggesting that creep strain at high temperatures cannot be disregarded if the experimental collapse behavior is to be reproduced. However, the calculated collapse time (dashed line) nearly agreed with the actual collapse time.

The bottom figures in Figs. 8 and 9 show that the calculated deflection W at the middle of the columns started to increase when axial displacement U started to contract.

4.2 Tests of Fire-resistant Steel Columns B-FR06 (Fig. 10) and B-FR10 (Fig. 11)

A fire-resistant steel column B-FR06 (Fig. 10) was heated by the ISO834 standard fire temperature curve, and B-FR10 (Fig. 11) was heated by the hydrocarbon fire curve. The existing load ratios to sustained allowable load were 0.6 for B-FR06 (Fig. 10) and 1.0 for B-FR10 (Fig. 11). The mean axial stress values, which were calculated by simply dividing the axial load by sectional area, were 143.3 N/mm^2 and 236.5 N/mm^2, respectively.

The upper figures in Figs. 10 and 11 show the steel temperatures measured at points on Level E (experimental values), and the middle and bottom figures show the column elongation (experimental and calculated values). The middle figures show the results of calculations made using values 40% larger and smaller than the ε_c value determined by Eq. (3). In the bottom figures, ε_c values 0.01, 0.1, 0.4, and 1.0 times the value determined by Eq. (3) were used.

The middle figures are calculations made to examine the effects of the accuracy of the creep-strain equation at high temperatures. The bottom figures show attempts to indirectly correct the equation using the results of loaded fire resistance tests of steel columns. In the middle and bottom figures, open circles denote the experimental values, solid lines denote values calculated by considering creep strain at high temperatures, and dashed lines denote calculations done by disregarding creep strain.

As shown in the upper figures, the temperature distribution was almost uniform throughout the cross-section when the columns were heated. The steel temperatures of B-FR06 and B-FR10 rose almost linearly by 150 °C to 200 °C per hour.

The calculated values with consideration of creep strain at high temperatures (solid line) reproduced the overall experimental behaviors after the contraction of axial deformation up to collapse. The 40% fluctuation of the creep strain at high temperatures caused smaller effects than in conventional steel (middle figures of Figs. 8 and 9). The experimental behaviors (open circles) shown in the middle figures in Figs. 10 and 11 and the behaviors calculated by considering creep strain at high temperatures (solid lines) differed in two respects.

The first difference was that the drops in elongation observed in the experiment at steel temperatures above 400 °C were not reproduced in the calculation. The other was that the calculation resulted in sudden collapse after axial deformation started to contract.

The first difference can be explained using creep curves of fire-resistant steel at 550 °C (lower figure of Fig. 7). In this study, the mean stresses of the columns were 143.3 to 236.5 N/mm^2, but at a stress level of 550 °C, the values calculated using Eq. (3) were much smaller than the experimental values.

In the lower figure of Fig. 7, the experimental values of fire-resistant steel (dashed lines) at 550 °C showed primary creep strain at the start of the experiment, followed by a gradual transition to secondary creep. On the other hand, the values calculated using the approximation equation did not reproduce the modes at the start of the experiment. Such a creep equation resulted in the underestimation of primary creep strain and thus resulted in almost no contraction of axial deformation (deceleration of elongation) by creep strain at high temperatures in the calculations shown in the middle figures of Figs. 10 and 11.

On the other hand, the latter difference was possibly attributable to an overestimation of the strain by Eq. (3), which yielded strain values larger than the actual strains of the columns.

As described in Section 3.3.3, the constants of Eq. (3) for calculating creep strain at high temperatures for analyzing fire-resistant steel NSFR490A were derived by "approximating the results of the ordinary creep test by the least squares method" (Reference [10]), not by conducting a creep experiment of SN490B-FR at high temperatures. Thus, the constants should be corrected by considering the significance of the constants of such a creep equation rather than by discussing in detail the differences between the experimental and calculated values in the middle figures of Figs. 10 and 11. In this study, the coefficients of Eq. (3) were indirectly corrected by analyzing the results of loaded fire resistance tests of steel tube columns.

The bottom portions of Figs. 10 and 11 show calculations made by setting the scale of Eq. (3) low (0.01 to 1.0) in an attempt to address the problem. When the creep strain ε_c value obtained by Eq. (3) was reduced, the collapse time was prolonged. At ε_c equal to 0.1 of the value of Eq. (3), the collapse time almost matched the experimental collapse time. Thus, the creep strain of fire-resistant steel SN490B-FR is possibly much smaller than the creep strain of NSFR490A, from which Eq. (3) was derived.

4.3 Collapse Time

The experimental and calculated collapse time values of all cases investigated in this study are compared in Fig. 12. In the figure, open circles denote the values calculated by disregarding the creep strain at high temperatures, and dark squares denote the values calculated by considering the creep strain at high temperatures, as determined using Eq. (3). The experimental collapse time was the time when the columns failed to sustain their axial load constant, and the calculated collapse time was when the convergence calculation could no longer be applied.

The figure shows that the calculated and experimental values differed by less than 10%. The analytical values calculated by considering the creep strain at high temperatures (dark squares) were on the safer side than the experimental values, and the values calculated by disregarding the creep strain (open circles) were on the dangerous side.

5. CONCLUSIONS

A non-linear numerical simulation analysis of the one-dimensional finite element method was conducted on loaded fire resistance tests of full-scale press-formed square steel tube columns, and the analytical results were compared with the experimental results. The study revealed the following:

(1) The calculation of the behaviors of BCP columns (B-CS06 and B-CS10) using conventional steel SN490B correctly reproduced the behaviors observed during the experiments and was found to make predictions on the safe side. Thus, the one-dimensional finite element calculation method used in this study appears to be valid. An equation for calculating creep strain at high temperatures for SM50A steel also appears to be feasible for predicting the behaviors of SN490 steel at high temperatures.

(2) Numerical analysis of B-FR06 and B-FR10 using fire-resistant steel NSFR490B columns did not reproduce the axial displacement behaviors of the columns before contraction and predicted much earlier collapse than the experiments did even when creep at high temperatures was considered. This problem may have occurred because the equation used to calculate creep strain at high temperatures underestimated the first-stage creep up to 550 °C and overestimated the creep at temperatures above 600 °C.

(3) A comparison of all the experimental and calculated collapse time values showed that the calculated values differed from the experimental values by less than 10%. The analytical values calculated by considering the creep behaviors at high temperatures were on a safer side than the experimental values, and the values calculated by disregarding the behaviors were on the dangerous side.

A simulation analysis of the results of loaded fire resistance tests of full-scale, press-formed square steel tube columns by numerical analysis showed the importance of obtaining creep property data of steel at high temperatures. To accurately predict the behaviors of steel structures and buildings at high temperatures, the creep properties of SN490C and fire-resistant steel should be experimentally confirmed.

6. REFERENCES

1. Kohno, M. and Masuda, H.: Fire-resistance of Large Steel Columns under Axial Load, Proc. of CIB-CTBUH International Conference on Tall Buildings, 2003.

2. Kohno, M., Sakumoto, Y., and Fushimi, M.: Effects of Large Section Size and Fire Resistant Steel on Redundancy Improvement of Steel High-rise Buildings in Fire, Proc. of the CTBUH 2004 Seoul Conference, 2004.
3. Okabe, T. and Kohno, M.: Numerical Simulation of Fire Resistance Test of Large Steel Columns under Axial Load, Journal of Structural Engineering, Vol. 51B, 2005.
4. Fujimoto, M., Wada, A., Shirakata, K., and Kosugi, T.: Non-linear Analysis of Braced Steel Frames, J. of Structural and Construction Engineering, Trans. of A.I.J., No. 209, 1973.
5. Furumura, F., Ave, T., Okabe, T., and Kim, W. J.: A Uniaxial Stress-strain Formula of Structural Steel at High Temperature and its Application to Thermal Deformation Analysis of Steel Frames, J. of Structural and Construction Engineering, Trans. of A.I.J., No. 363, 1986.
6. Furumura, F., Migita, K., Takeo, A., Okabe, T., and Kim, W. J.: Elasto-plastic Creep Thermal Deformation Behavior of Plastic Designed Steel Frames, J. of Structural and Construction Engineering, Trans. of A.I.J., No. 368, 1986.
7. Furumura, F., Ave, T., Kim, W. J., and Okabe, T.: Nonlinear Elasto-plastic Creep Behavior of Structural Steel under Continuously Varying Stress and Temperature, J. of Structural and Construction Engineering, Trans. of A.I.J., No. 353, 1985.
8. Fujimoto, M., Furumura, F., and Ave, T.: Primary Creep of Structural Steel (SM50A) at High Temperatures, J. of Structural and Construction Engineering, Trans. of A.I.J., No. 306, 1981.8.
9. Kuwamura, H., Akiyama, H., Yamada, S., and Jung-Cheng, C.: Experiment on the Mechanical Properties and Their Improvement of Cold Press-Bent Steel Plates, J. of Structural and Construction Engineering, Trans. of A.I.J., No. 444, 1993.2.
10. Sakumoto, Y., Yamaguchi, T., Ohashi, M., and Saito, H.: High-temperature Properties of Fire-resistant Steel FR Buildings, ASCE, Journal of Structural Engineering, Vol. 118, No.2, 1992.
11. Sakumoto, Y., Yamaguchi, T., Okada, T., Yoshida, M., Tasaka, S., and Saito, H.: Experimental Study for Fire Resistance of Fire Resistant Steel Columns, J. of Structural and Construction Engineering, Trans. of A.I.J., No. 434, 1992.
12. Okabe, T., Sakumoto, Y., Okabda, T., and Yamaguchi, T.: Calculation of Fire Resistance Tests on Concrete-filled Steel Tube Columns using FR Steel, Journal of Structural Engineering, Vol. 40B, 1994.
13. Hirayama, H. et al.: Fire Resistance of Protected Steel Column, Summaries of Technical Papers of Annual Meeting, Architectural Institute of Japan, A-2, 2000.
14. Okabe, T. and Ave, T.: Buckling Strength of Steel Columns using Structural Steel (SN490B) at High Temperature, J. of Structural and Construction Engineering, Trans. of A.I.J., No. 585, 2004.11.

Table 1 Parameters of Steel Columns (Reference [2])

	Symbol (Unit)	Series B
Section Shape	Press Formed □-600 × 600 × 28	
Specified Design Strength	F (N/mm^2)	325
Cross-sectional Area	A (mm^2)	6.00×10^4
Length	L (mm)	4 300
Second Inertia	I (mm^4)	3.14×10^9
Slenderness Ratio	λ	18.8
Shape Factor	Hp/A (m^{-1})	39.0
Weight	W (kg)	2.03×10^3

Table 2 Summary of Experiment Series B (Reference [2])

Symbol	Steel Grade	Fire Protection	Applied Load (Ratio*)	Heating Curve
B-CS06	SN490B CP325	Ceramic fiber blanket 30 mm (Fireguard C-60)	8.60 MN (0.6)	ISO-834
B-FR06	SN490B-FR BCP325		8.67 MN (0.6)	ISO-834
B-CS10	SN490B BCP325		14.19 MN (1.0)	Hydrocarbon
B-FR10	SN490B-FR BCP325		14.45 MN (1.0)	Hydrocarbon

* Load ratio to the sustained allowable load.

Table 3 Mechanical Properties (mill sheet)

Test Piece (Plate 28 mm)	σ_{yRT} (N/mm^2)	σ_{uRT} (N/mm^2)	Elong.$_{RT}$ (%)
SN490B	363	522	31
SN490B-FR	389	577	24

Table 4 Coefficients of Stress-strain Curves (SN490B)

Temp. (°C)	$\frac{E_T}{E_{RT}}$	$\frac{\sigma_{0T}}{\sigma_{yRT}}$	n_{oT}	$\frac{E_T - E_{pT}}{E_{RT}}$	$\frac{\sigma_T}{\sigma_{yRT}}$	n_T
RT	1.000	1.000	82	0.992	1.246	0.849
200	0.887	0.752	3.32	0.869	1.046	1.073
400	0.865	0.568	4.719	0.844	0.846	1.480
500	0.710	0.050	4.719	0.698	0.703	1.499
600	0.549	0.050	4.719	0.545	0.475	1.766
700	0.307	0.050	4.719	0.306	0.258	2.721

T: temperature, RT: ambient temperature, E: Young's modulus, σ_y: yield strength

Table 5 Coefficients of Stress-strain Curves (SN490B-FR)

Temp. (°C)	$\frac{E_T}{E_{RT}}$	$\frac{E_T - E_{pT}}{E_{RT}}$	$\frac{\sigma_T}{\sigma_{yRT}}$	n_T
RT	1.000	0.989	1.151	2.077
300	0.933	0.924	1.280	1.387
400	0.894	0.885	1.204	1.485
500	0.833	0.832	1.185	1.409
600	0.809	0.809	0.864	1.870
700	0.608	0.608	0.433	1.567
800	0.238	0.238	0.216	3.109

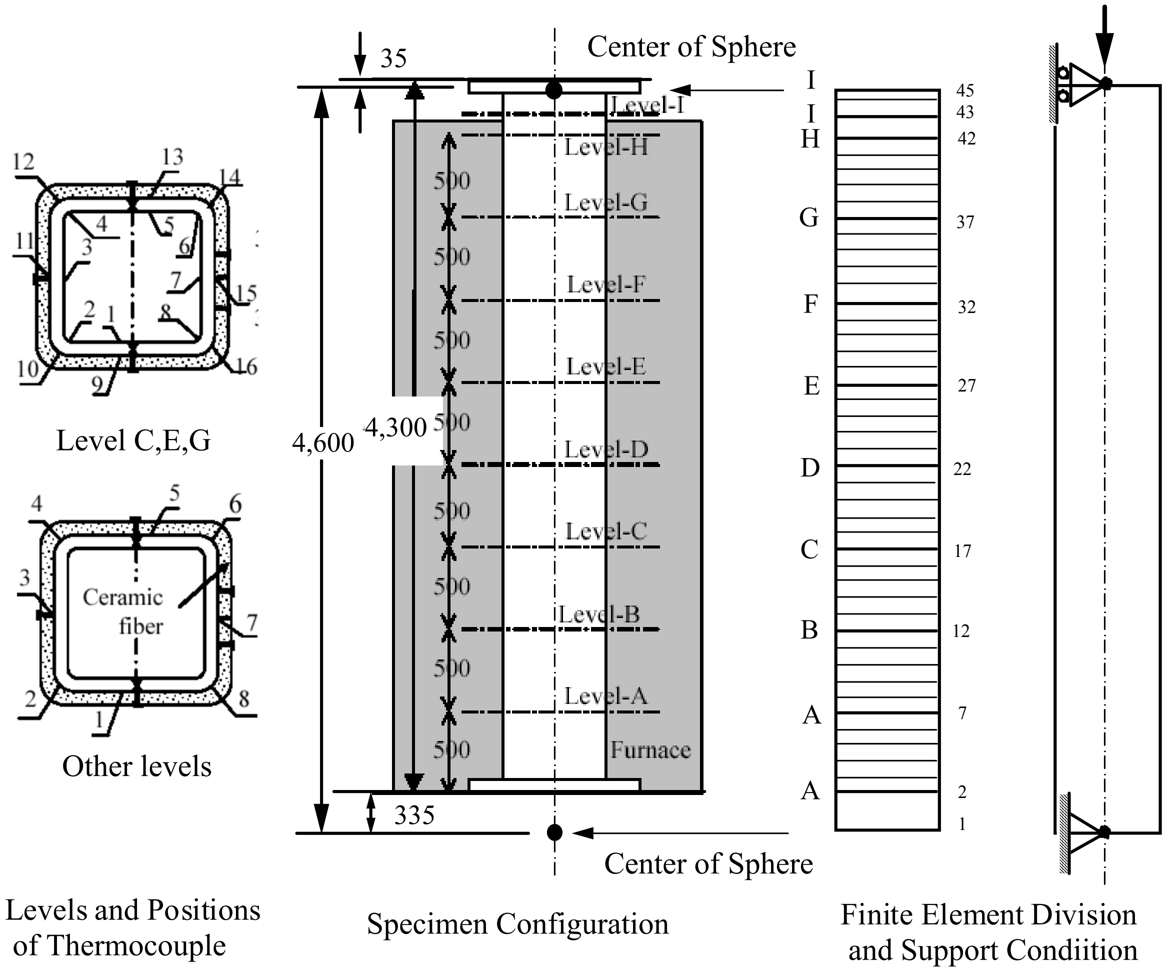

Fig. 1 Analytical Model of Fire Resistance Test

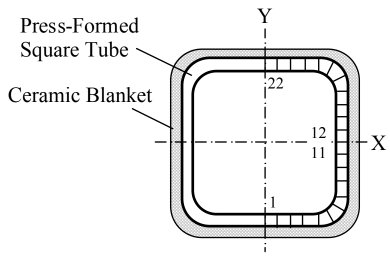

Fig. 2 Sectional Division

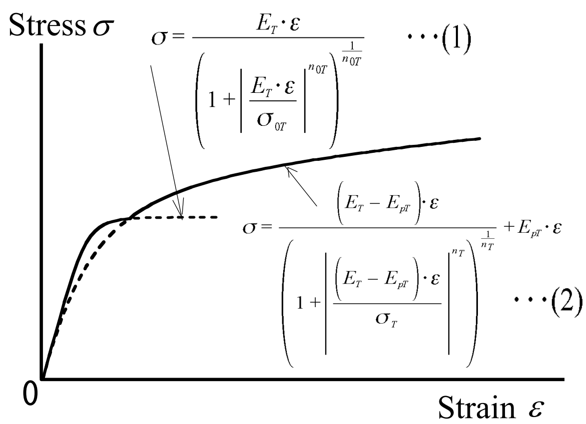

Fig. 3 Equations of Stress-Strain Relationship

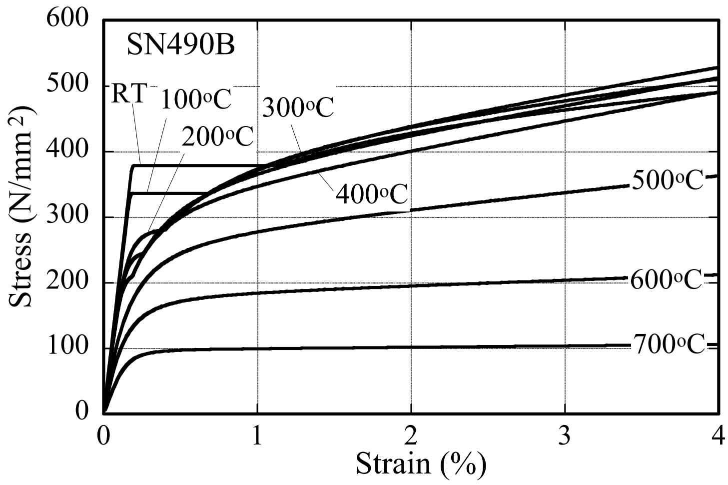

Fig. 4 Stress-Strain Relationship (SN490B)

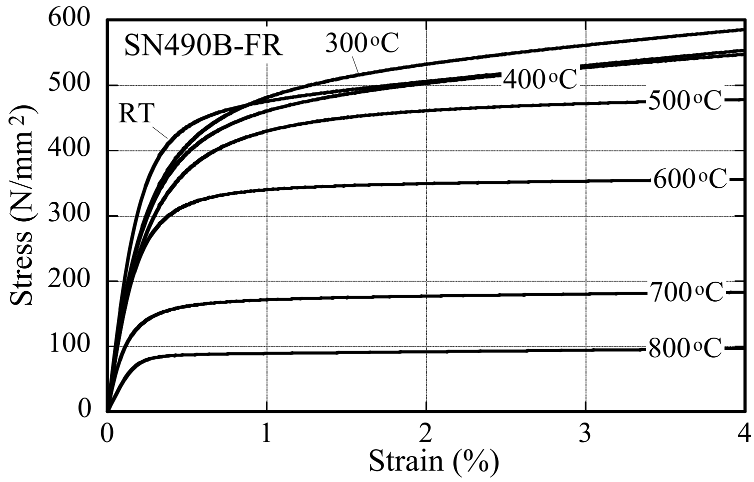

Fig. 5 Stress-Strain Relationship (SN490B-FR)

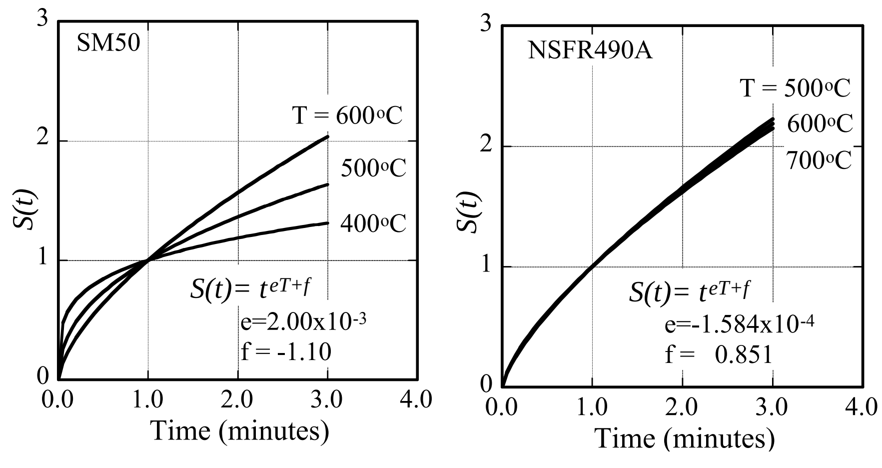

Fig. 6 Profile of time term t^{eT+f}

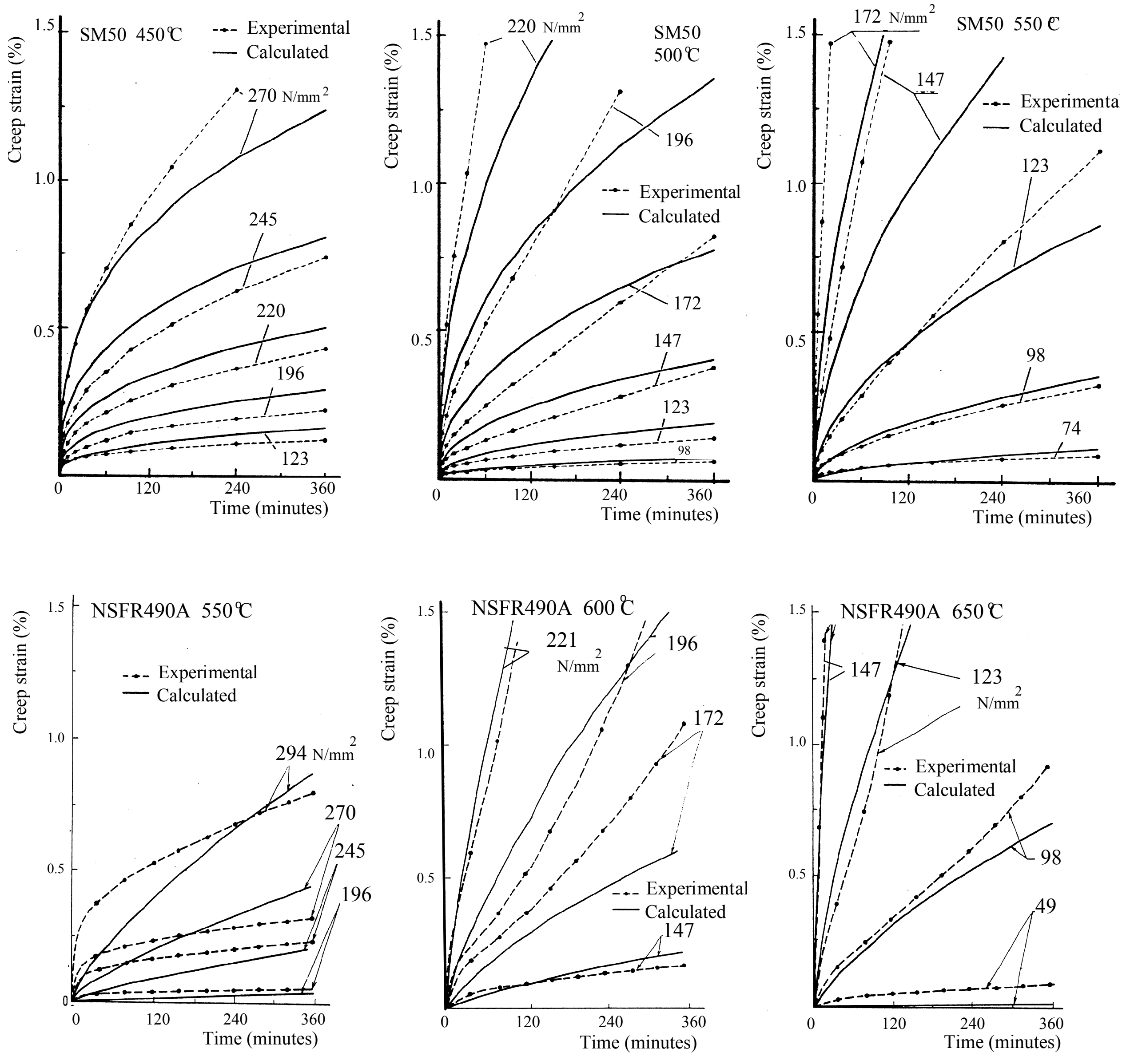

Fig. 7 Experimental creep strain (References [8, 10])

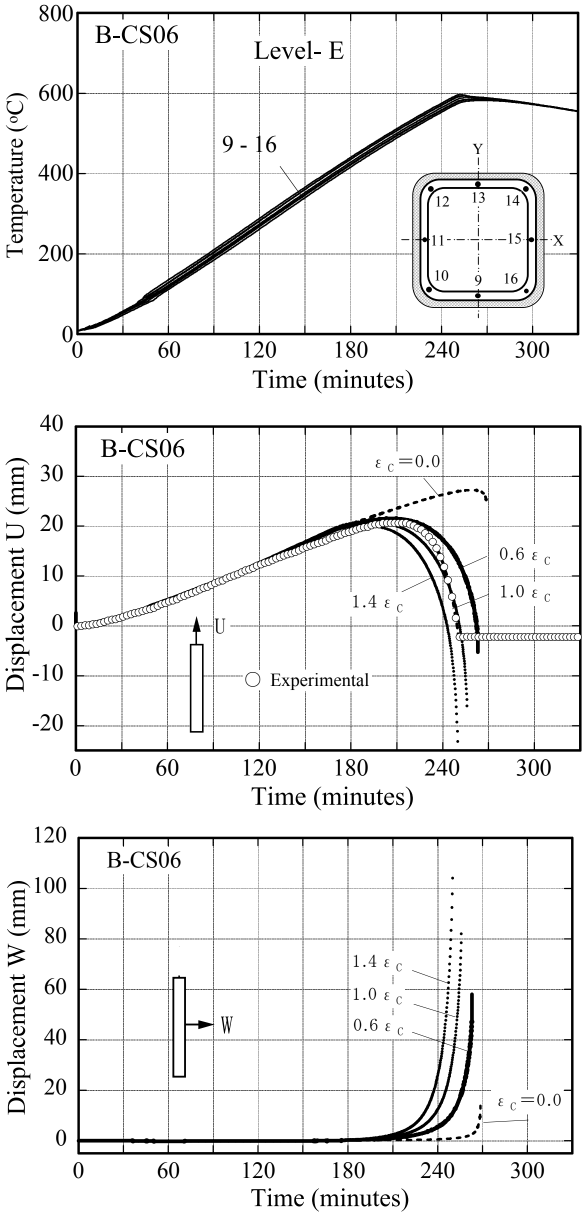

Fig. 8 Experimental and Calculated Values (B-CS06)

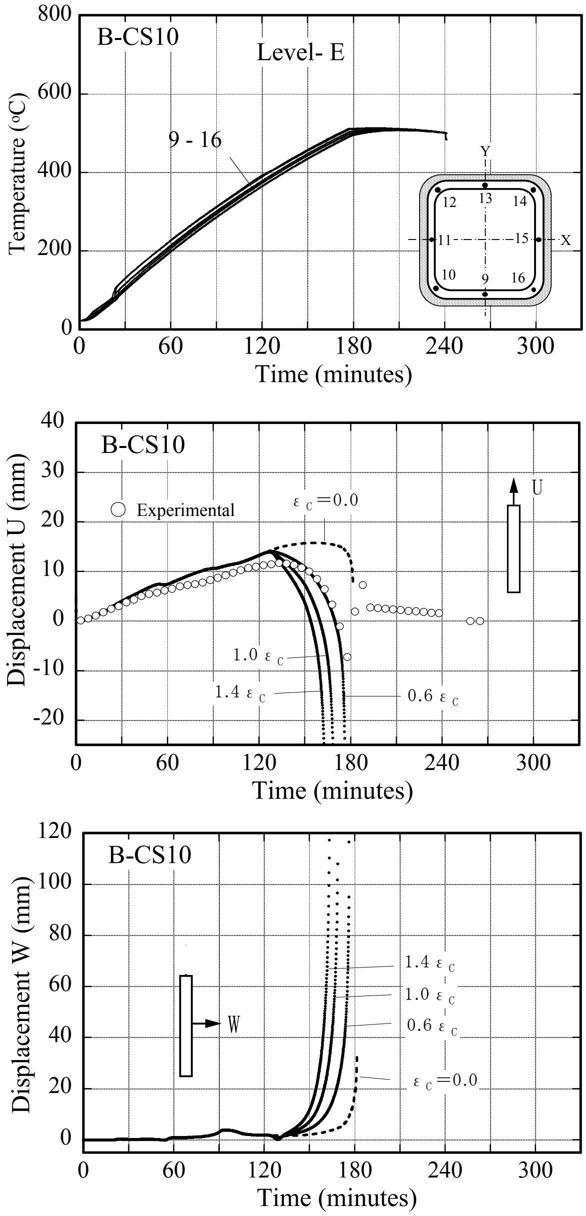

Fig. 9 Experimental and Calculated Values (B-CS10)

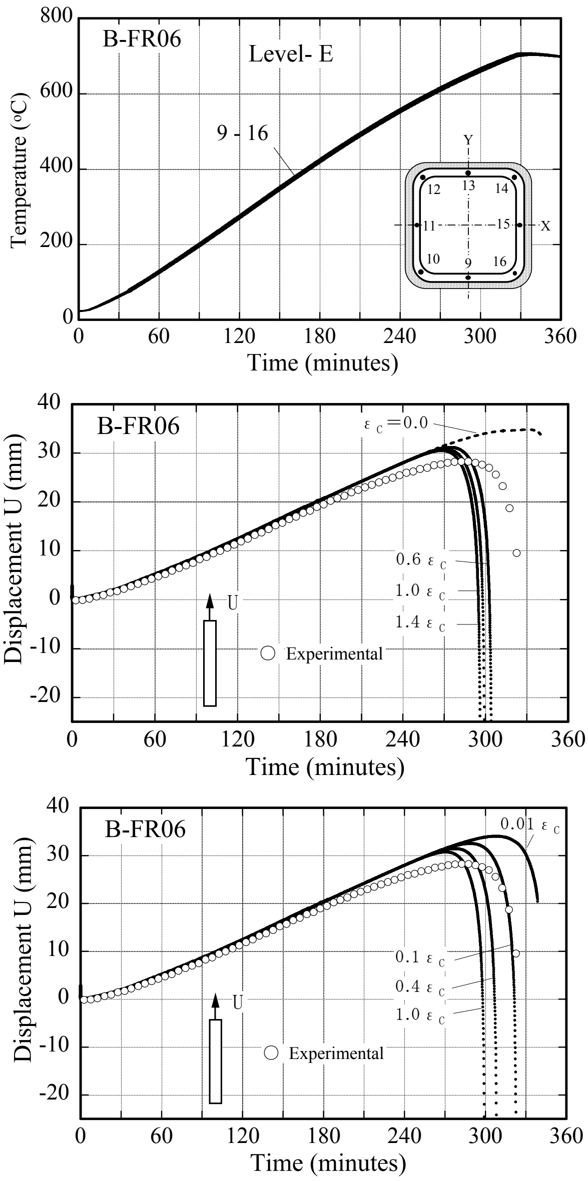

Fig. 10 Experimental and Calculated Values (B-FR06)

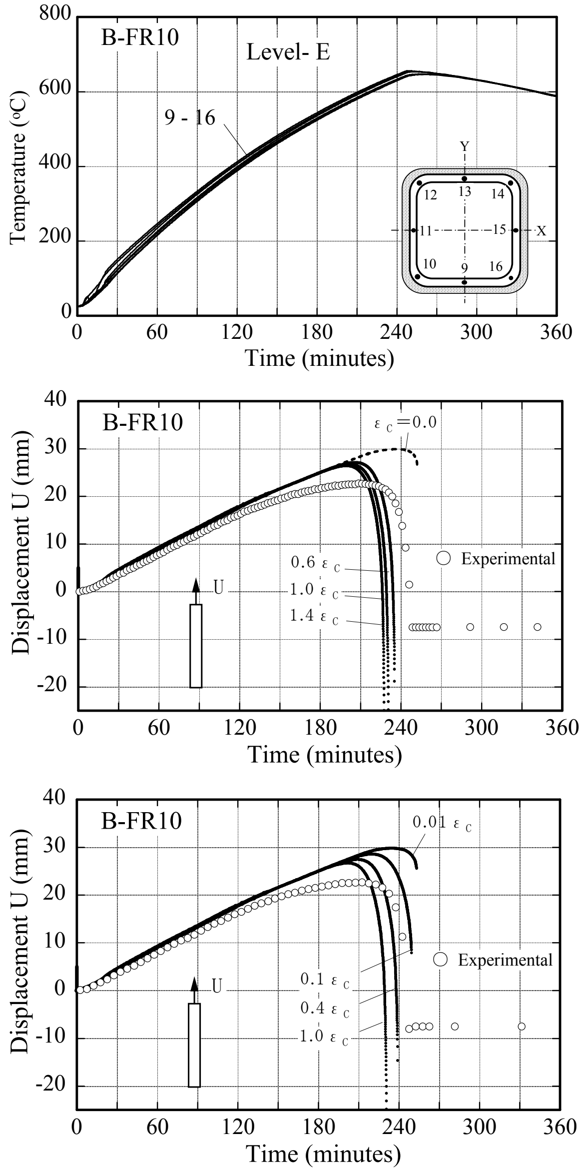

Fig. 11 Experimental and Calculated Values (B-FR10)

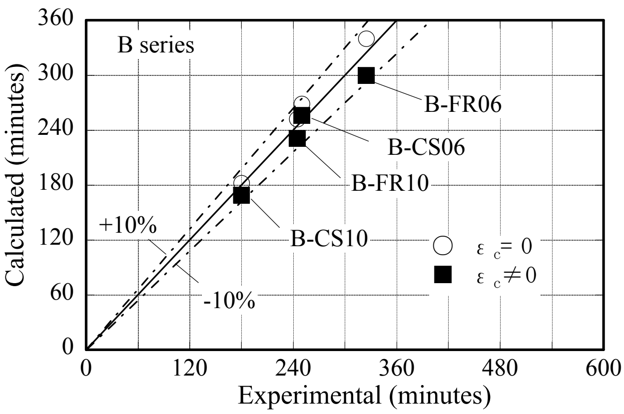

Fig. 12 Collapse Time